Interaction of Amoebapores and NK-Lysin with Symmetric Phospholipid and Asymmetric Lipopolysaccharide/Phospholipid Bilayers†

Thomas Gutsmann,*,‡ Beate Riekens,§ Heike Bruhn,|| Andre Wiese,‡ Ulrich Seydel,‡ and Matthias Leippe||

Research Center Borstel, Center for Medicine and Biosciences, Department of Immunochemistry and Biochemical Microbiology, Parkallee 10, D-23845 Borstel, Germany, Bernhard Nocht Institute for Tropical Medicine, Parasitology Section, Bernhard-Nocht-Strasse 74, D-20359 Hamburg, Germany, and Molecular Parasitology Group, Research Center for Infectious Diseases, Röntgenring 11, D-97070 Würzburg, Germany

Received April 29, 2003; Revised Manuscript Received June 13, 2003

ABSTRACT: Amoebapores from protozoan parasite *Entamoeba histolytica* and NK-lysin of porcine cytotoxic lymphocytes belong to the same family of saposin-like proteins. In addition to the structural similarity, amoebapores and NK-lysin are both highly effective against prokaryotic and eukaryotic target cells in that they permeabilize the target cell membranes. Here, we have investigated in detail the protein/lipid interaction for the three isoforms of amoebapore and NK-lysin. Results obtained from electrical measurements on planar bilayer membranes, including reconstitution models of the lipid matrix of the outer membrane of *Escherichia coli* and phospholipid membranes, fluorescence energy transfer spectroscopy with liposomes, and monolayer measurements on a Langmuir trough, provided information on lipid preferences, pH dependences, and membrane interaction mechanisms. The three amoebapores led to the formation of transient pores with similar characteristics in conductance, sublevels, and lifetime for the different isoforms. The conductance of the pores was dependent on the polarity of the applied clamp voltage, and the distribution of the sublevels was affected by the value of the clamp voltage. The size of the pores and distribution of conductance sublevels differed between symmetric phospholipid and asymmetric lipopolysaccharide/phospholipid bilayers. Notably, NK-lysin caused the formation of well-defined pores, which were lipid- and voltage-dependent, and their characteristics differed from those induced by amoebapores; e.g., the protein concentration necessary to induce pore formation was 20 times higher. The biophysical data give important information on the mode of action of these small effector proteins, which may further lead to a better understanding of peptide-membrane interactions in general.

Natural antimicrobial and cytolytic peptides have attracted considerable interest during recent times due to their potential use as leads for new antibiotics and tumoricidal therapeutics. In animal and plants, such peptides play an important role in the internal defense against various microbes. Although a variety of models about their mode of action have been described, it is the consensus view that the first target of the vast majority of antimicrobial peptides is the cell envelope or cell membrane, which they have to permeate (for a review see ref *1*). In contrast to the "classical" antibiotics in therapeutic use, resistances have not been observed, and it is likely that the risk that microbes become resistant against natural antimicrobial peptides is small because of their preference for microbial membranes as a target and their existence as effective weapons in nature for millions of years. Typically, these peptides consist of 10−40 amino acid residues. A particular group of polypeptides are produced by porcine and human cytotoxic lymphocytes, which have a size of 74−78 residues and are termed NK-lysin and granulysin (*2*, *3*). Interestingly, the archetype of this peptide class exists in amoebae: the pore-forming proteins of pathogenic *Entamoeba histolytica*, termed amoebapores (*4*). The amoebapores (AP)[1] exist in three isoforms, A, B, and C, all of a length of 77 residues but displaying considerable sequence diversity (*5*−*8*). Structurally, NK-lysin, granulysin, and the amoebapores belong to the same protein family, the saposin-like proteins (SAPLIPs) (*9*). The 3D structure of the SAPLIPs is globular and comprises a bundle of five mostly amphipathic helices connected by three conserved disulfide bonds, as evidenced first for NK-lysin (*10*). Although their members display diverse biological activities, a common property of the SAPLIP family is the ability of the proteins to interact with lipids.

Functionally, NK-lysin, granulysin, and amoebapores have in common that they possess antibacterial activity, which in

† This work was financially supported by the Deutsche Forschungsgemeinschaft (LE 1075/2-3; SFB 470, Project B5; SFB 617, Project A17; and GU 568/2-1).

* Corresponding author. Present address: University of California Santa Barbara, Physics Department, Santa Barbara, CA, 93106. Phone: +1 (805) 893 3999. Fax: +1 (805) 893 8315. E-mail: tguts@physics.ucsb.edu.

‡ Research Center Borstel.

§ Bernhard Nocht Institute for Tropical Medicine.

|| Research Center for Infectious Diseases.

[1] Abbreviations: AP, amoebapore; DPG, diphosphatidylglycerol; DPhyPC, diphytanoylphosphatidylcholine; FRET, Förster/fluorescence resonance energy transfer; LPS, lipopolysaccharide; NBD-PE, N-(7-nitro-2;1;3-benzoxadiazol-4-yl)-PE; PC, phosphatidylcholine; PE, phosphatidylethanolamine; PG, phosphatidylglycerol; PL, phospholipid mixture; PS, phosphatidylserine; Rh-PE, N-(rhodamine B sulfonyl)-PE.

10.1021/bi034686u CCC: $25.00
Published on Web 07/25/2003

mammals permits the defense against invading microbes (*2*, *11*) and which the amoeba apparently uses to kill phagocytosed bacteria (*12*). Moreover, NK-lysin and amoebapores are cytolytic to eukaryotic cells as well, which makes the latter an important constituent of the tissue-destructive armament of the pathogenic amoebae (*13*). Their mode of action is membrane permeabilization ("pore formation") after binding to phospholipids, and hence activity does not depend on the interaction with a specific membrane receptor.

Amoebapores and NK-lysin show only limited sequence homology. And a detailed analysis of the known structure of NK-lysin and models derived therefrom for the amoebapores revealed significant structural differences despite their common fold (*14*). When the biological activities are compared, differences also become apparent. In contrast to NK-lysin, the amoebapores exhibited a pronounced dependence of all their activities on acidic pH (*8*). Whereas amoebapores are more potent against Gram-positive than against Gram-negative bacteria (*7*, *12*), NK-lysin appears to have no preference. (*2*).

In this work, we focused on an understanding of the pore formation of the three isoforms of amoebapore and of NK-lysin in different artificial lipid membranes resembling those of various cell types but with particular emphasis on Gram-negative bacteria. The first target of all antibacterial peptides is the bacterial cell envelope, and in case of Gram-negative bacteria, the outer membrane (*15*). This outer membrane is an extremely asymmetric bilayer with respect to the lipid composition. With some exceptions, the outer leaflet of this bilayer consists of lipopolysaccharide (LPS) (*16*) carrying negatively charged groups, which results in a relatively high negative surface charge density. The inner leaflet is composed of a phospholipid mixture (*17*).

To investigate the interaction of peptides—in particular, of pore-forming peptides—with membranes, reconstitution models of lipid matrixes are very helpful. Planar lipid bilayers are an important tool for such studies (*18*−*21*). Using the method of Montal and Mueller (*22*), it is possible to reconstitute the asymmetric outer membrane of Gram-negative bacteria (*23*). Here, we show results obtained from experiments using planar lipid bilayers, liposomes, and monolayers composed of various (glyco-)lipids.

Early studies describe the induction of ion channel formation in artificial membranes by amoebic extracts or partially purified amoebapore. Lynch et al. showed that a protein from *E. histolytica* induced the formation of pores in planar bilayers composed of azolectin or diphytanoylphosphatidylcholine (DPhyPC) with a unit conductance of (1.6 ± 0.2) nS in 1 M KCl (*24*). Furthermore, they pointed out that the current response was linear in a range of −10 to −40 mV. In another study it was described that the formation of the pores was stimulated by the applied membrane potential, pores were rectifying, and the open-state probability increased strongly with pH (*25*). The characteristics of amoebapore channels are reported to be in accordance with the barrel-stave model that describes the creation of a transmembrane pore by insertion and oligomerization of protein monomers to a water-filled channel. In contrast, NK-lysin appears to permeabilize membranes without adopting a transmembrane orientation. So far, well-defined NK-lysin pores were not observed (*26*), and on the basis of that, a model of "molecular electroporation" has been proposed (*27*).

Here, we report that the three amoebapores led to the formation of transient, lipid- and voltage-dependent pores with comparable characteristics in conductance, sublevels, and lifetime for the different isoforms. The lipid dependence actually appears to be a charge density dependence because the amoebapores interact significantly stronger with negatively charged lipids. In contrast to others, we observed that NK-lysin caused the formation of well-defined pores, which were lipid- and voltage-dependent as well; however, their characteristics differed from those induced by amoebapores. Furthermore, the protein concentration necessary to induce pore formation had to be significantly higher.

MATERIAL AND METHODS

Lipids, Peptides, and Other Chemicals. For the formation of planar membranes, monolayers, and liposomes, deep rough mutant LPS from *Escherichia coli* strain F515 (F515 LPS) (chemical structures according to ref *28*) was used. LPS was extracted by the phenol/chloroform/petroleum ether method (*29*), purified, lyophilized, and transformed into the triethylamine salt form.

Phosphatidylethanolamine (PE) from bovine brain (type I), phosphatidylglycerol (PG) and phosphatidylcholine (PC) from egg yolk lecithin (sodium salt), and diphosphatidylglycerol (DPG) from bovine heart (sodium salt) were from Sigma (Deisenhofen, Germany), and phosphatidylserine (PS) and diphytanoylphosphatidylcholine (DPhyPC) were from Avanti Polar Lipids (Alabaster, AL). All phospholipids were used without further purification. The fluorescent dyes N-(7-nitro-2,1,3-benzoxadiazol-4-yl)-PE (NBD-PE) and N-(rhodamine B sulfonyl)-PE (Rh-PE) were purchased from Molecular Probes (Eugene, OR).

Amoebapores were purified from trophozoites of *E. histolytica* according to a procedure described previously using reversed-phase HPLC as the final step to separate individual isoforms (*7*, *30*). NK-lysin was expressed recombinantly in *E. coli* according to Jacobs et al. (*31*). The sequences of the proteins were validated by MALDI-TOF analysis and N-terminal protein sequencing. The structural integrity of recombinant NK-lysin has been verified by CD analysis. It reveals the spectrum of a helical protein devoid of β-structures; the content of α-helices were calculated to 49%, which is in good agreement with the known three-dimensional structure containing 52% α-helix (*10*). Moreover, no free sulhydryl groups have been detected using Elman's reagent (*32*), which clearly indicates the presence of three disulfide bonds. The peptides were stored in 0.01% trifluoroacetic acid (TFA) in a concentration of 1 mg/mL.

Four different bathing solutions (subphases) were used in the various experiments. All subphases contained 100 mM KCl and were used at a temperature of 37 °C. The subphases contained in addition the following: subphase 1 (specific electrical conductivity σ = 16.3 mS/cm), 8 mM sodium citrate (NaCi), pH 5.2; subphase 2 (σ = 17.2 mS/cm), 5 mM $MgCl_2$, 8mM NaCi, pH 5.2; subphase 3 (σ = 16.5 mS/cm), 5 mM HEPES, pH 7.0; subphase 4 (σ = 17.3 mS/cm), 5 mM $MgCl_2$, 5 mM HEPES, pH 7.0.

Preparation of Planar Bilayers and Electrical Measurements. Planar bilayers were prepared according to the Montal−Mueller technique (*22*) as described before (*33*, *34*). For the formation of bilayer membranes, natural phospho-

lipids and DPhyPC were dissolved in chloroform (2.5 mg/mL) and LPS in chloroform/methanol (10:1 v/v) (2.5 mg/mL). The phospholipid mixture PL consisted of a mixture of PE, PG, and DPG in molar ratios of 80:15:5, resembling the phospholipid composition of the inner leaflet of the outer membrane (*35*). In short, bilayers were formed by opposing two lipid monolayers prepared on aqueous subphases (bathing solutions) from chloroformic solutions of the lipids at a small aperture (typically 150 μm diameter) in a thin Teflon septum (12.5 μm thickness).

For electrical measurements, planar membranes were voltage-clamped, and the compartment opposite (trans compartment) where the peptide was added (cis compartment) was grounded. Therefore, in comparison to the natural system, a positive clamp voltage represents a membrane, which is negative on the inner side. Current is defined positive when cation flux is directed toward the grounded compartment. For the determination of the single fluctuation amplitudes, the current traces were filtered at a corner frequency of 1 kHz and digitized with a sampling frequency of 3 kHz. Peptides were added to the cis-side (named first) of the bilayer, e.g., to the F515 LPS side of an asymmetric F515 LPS/PL bilayer.

The determination of the membrane capacitance yields information on area, thickness, and composition of the bilayer. Membrane capacitance can be determined by applying steplike voltage pulses and measuring the resulting transient charging currents (*36*). In our setup, the capacitance was determined at a frequency of 1 Hz and a maximum clamp voltage of 1 mV. Accordingly, we were able to judge membrane qualities and to analyze membrane protein interactions without influencing the system by other agents such as carriers or by high clamp voltages.

Förster/Fluorescence Resonance Energy Transfer Spectroscopy. The Förster/fluorescence resonance energy transfer (FRET) spectroscopy was used as a probe dilution assay (*37*) to obtain information on the intercalation of the peptides into liposomes made from PC, PS, and LPS. For the FRET measurements, the various liposomes were double-labeled with NBD-PE and Rh-PE. The fluorescent dyes were dissolved together with PC, PS, or F515 LPS in chloroform in molar ratios [lipid]:[NBD-PE]:[Rh-PE] of 100:1:1. The solvent was evaporated under a stream of nitrogen, and the lipids were resuspended in the different bathing solutions, mixed thoroughly, and sonicated with a Branson sonicator for 1 min (1 mL solution). Subsequently, the preparation was cooled at 4 °C for 30 min, heated at 56 °C for 30 min, and recooled to 4 °C. Preparations were stored at 4 °C overnight prior to measurement. A preparation of 900 μL of the double-labeled phospholipid or LPS liposomes (10 μM) at 37 °C was excited at 470 nm (excitation wavelength of NBD-PE), and the intensities of the emission light of the donor NBD-PE (531 nm) and acceptor Rh−PE (593 nm) were measured simultaneously on a fluorescence spectrometer (SPEX F1T11, SPEX Instr., Edison, NY). The peptides were added after 50 s to a final concentration of 1 μg/mL. Intercalation were detected as changes in fluorescence intensities as a function of time (increase of donor signal, decrease of acceptor signal). In the following, the quotient of the donor and the acceptor intensities is denoted as the FRET signal.

Film Balance Measurements. From pressure/area isotherms of monolayers at the air/water interface of a film balance, the area of the composing molecules, lipids, and/or proteins, can be calculated at a given lateral pressure.

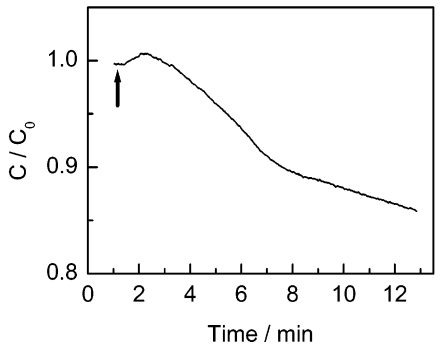

FIGURE 1: Changes in membrane capacitance induced by the major amoebapore isoform AP-A. Normalized capacitance vs time after addition of 0.5 μg/mL (60 nM) AP-A to a symmetric DPhyPC/DPhyPC bilayer. Bathing solution: 100 mM KCl, 5 mM $MgCl_2$, 8 mM NaCi, pH 5.2, T = 37 °C. An arrow marks the addition of AP-A.

The incorporation of the peptides into lipid monolayers dependent on the composition of the aqueous subphase was studied with monolayers spread from a 1 mM solution of PS in chloroform or a 1 mM solution of F515 LPS in chloroform/methanol (9:1 v/v) solutions. Subsequently, the experiments were conducted as described earlier (*38*).

RESULTS

Influence of the Peptides on Capacitance and Conductance of Planar Bilayers. Membrane Capacitance. Changes in membrane capacitance after addition of peptides are indicative of their interaction, e.g., binding or intercalation, with the lipid bilayer prior to a possible permeabilization of the membrane.

Each of the three isoforms of amoebapore (AP) as well as NK-lysin (NK-L) induced changes of the membrane capacitance of PL/PL, LPS/PL, and even electrically neutral DPhyPC/DPhyPC membranes (Figure 1). Qualitatively, the capacitance curves had the same run: after a slight increase the capacitance decreased in a concentration-dependent manner. Quantitatively, the addition of 1μg/mL AP-A to a PL/PL membrane resulted in a fast decrease and finally to a disruption of the bilayer. NK-L in the same concentration led to a slower decrease of the capacitance. Accordingly, approximately 10 times higher amounts of NK-L were needed to induce effects similar to those observed upon addition of AP-A. This parameter appeared to be not significantly affected by the composition of the membranes or the subphases.

Membrane Conductance. For determination of the membrane integrity, the conductance is the most important parameter. An intact, undisturbed, and solvent-free bilayer has a negligible electrical conductance of <1 pA. Peptides may cause transient or permanent lesions/pores, which lead to an increase in membrane conductance.

First, we investigated the influence of amoebapores on the conductance of symmetric PL/PL bilayers. The addition of approximately 5 nM of each of the isoforms led to an induction of transient current fluctuations caused by pores with comparable characteristics with respect to size and lifetime (Figure 2). The peptides formed distinct transient pores with lifetimes in the range of seconds and

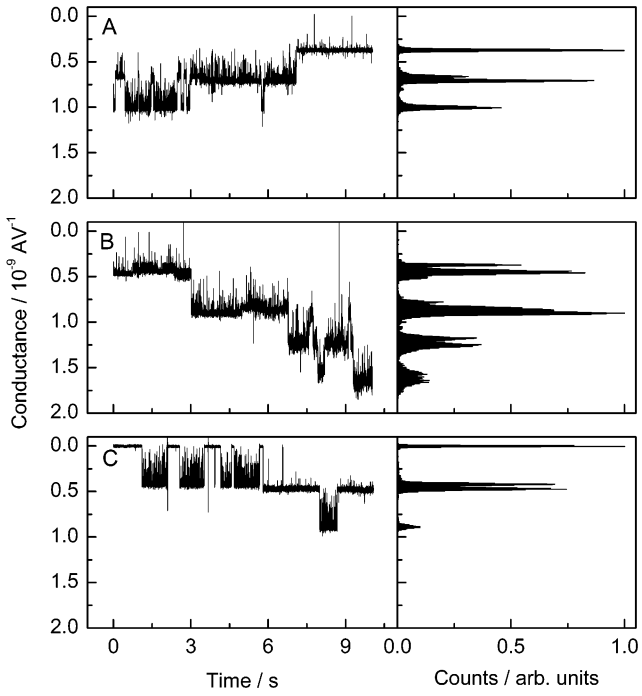

FIGURE 2: Current fluctuations in symmetric PL/PL bilayers induced after the addition of different amoebapore isoforms: (A) 6 nM AP-A, (B) 3 nM AP-B, or (C) 6 nM AP-C. The clamp voltage was −40 mV (trans side grounded) in all experiments. Left side, time course; right side, respective amplitude histogram. Bathing solution: 100 mM KCl, 5 mM $MgCl_2$, 8 mM NaCl, pH 5.2, T = 37 °C.

preferential conductance levels. The conductance was independent from the value of the negative clamp voltage (negative on the side of peptide addition). Assuming a circular geometry of the pores and a membrane thickness of $l = 6$ nm, the mean diameter d of the pores was calculated according to the simple relation $I = (\pi\sigma d^2 U)/(4l)$, with I being the mean current, σ the specific conductance of the subphase, and U the clamp voltage, and the following results were obtained: $d_{AP-A} = (1.22 \pm 0.14)$ nm, $d_{AP-B} = (1.25 \pm 0.07)$ nm, and $d_{AP-C} = (1.29 \pm 0.06)$ nm. However, also sublevels were observed (Figures 2 and 3, trace B), and their number and frequency increased with increasing negative clamp voltages. On the basis of these data, it could not be distiguished whether these sublevels in the conductance resulted from additional smaller pores or from sublevels in pore size.

When a positive clamp voltage was applied, in rare cases pores with similar characteristics were observed; however, in most cases the conductances and lifetimes of the pores were significantly smaller (Figure 3). Minimal clamp voltages for pore formation could not be determined; even voltages of ±10 mV were sufficient.

As described earlier (*8*, *12*), the pore-forming and antimicrobial activity of the amoebapores is pH-dependent with an optimum at acidic pH (5.2), and only inferior activity is displayed at neutral pH. One possible explanation for this observation would be an alteration of the pore characteristics or a reduced pore formation. However, we could not observe any change in conductance and lifetime of the pores when changing the pH of the subphase from 5.2 to 7.0, and also, the peptide concentrations needed did not differed significantly (data not shown).

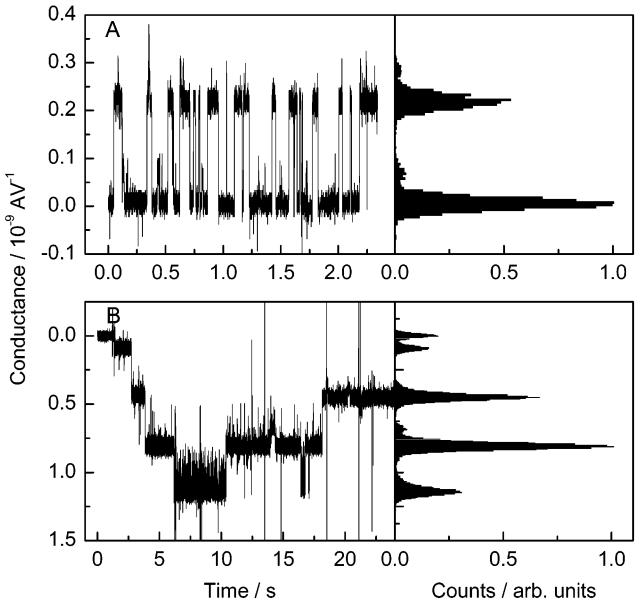

FIGURE 3: Current fluctuations in a symmetric PL/PL bilayer induced by the addition of 3 nM AP-A. Trace A, clamp voltage of +20 mV (trans side grounded); trace B, clamp voltage of −20 mV. Left side: time course; right side: respective amplitude histogram. Bathing solution: 100 mM KCl, 5 mM $MgCl_2$, 8 mM NaCl, pH 5.2, T = 37 °C.

Amoebapores are at significantly lower concentrations active against Gram-positive than against Gram-negative bacteria, although they do permeabilize the outer membrane of the latter (*12*). To analyze the molecular basis of this target cell preference, we determined the pore forming activity of the amoebapores on reconstituted membranes composed of the lipopolysaccharide F515 LPS on the side of peptide addition and the phospholipid mixture PL on the inner leaflet. We applied a clamp voltage of 26 mV, according to that determined by Sen et al. (*39*) for the outer membrane of *E. coli* in the presence of an external cation concentration of 100 mM and observed an increase of membrane conductance after addition of each of the amoebapore isoforms (data not shown). Application of negative clamp voltages resulted in the formation of pores with characteristics comparable to those of pores induced in PL/PL membranes. Interestingly, most of the pores induced at positive clamp voltages had different characteristics. Figure 4A shows a conductance trace after addition of AP-A to a F515 LPS/PL membrane. From the detail B of this trace (Figure 4B), it can be seen that AP-A is able to form large pores with at least two sublevels, which would correspond to a pore diameter of 1.33 and 2.21 nm, respectively. Detail C (Figure 4) shows a small pore with a calculated diameter of only 0.63 nm and a lifetime of 33 ms. Detail D (Figure 4) shows a pore with a diameter of 1.15 nm, which was in an open state most of the time but also changed to a closed state or lower conductance level for less than 1 ms. Collectively, AP-A induces the formation of pores in F515 LPS/PL membranes, the diameters, sublevels, and lifetimes of which may vary considerably. AP-B and AP-C also leads to the formation of pores with various characteristics in F515 LPS/PL membranes. Figure 5 shows an interesting conductance trace of AP-B pores containing three repetitions of the same motif, which is shown in the inset in more detail. Here it became apparent that the pores most likely exist in different conformations,

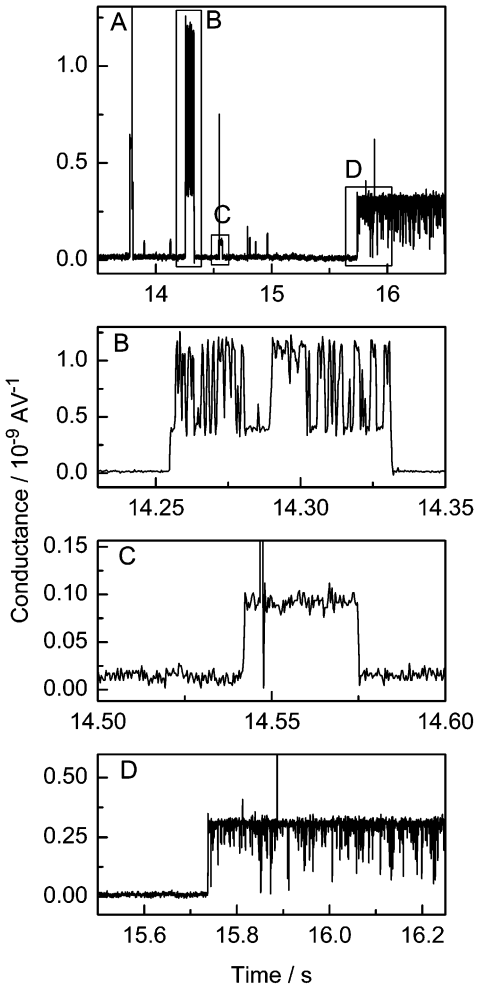

FIGURE 4: Current fluctuations after addition of 3 nM AP-A to the LPS side of a F515 LPS/PL bilayer at a clamp voltage of +40 mV. Trace A, overview of different types of current fluctuations; traces B, C, and D, respective details of trace A. Bathing solution: 100 mM KCl, 5 mM $MgCl_2$, 8 mM NaCi, pH 5.2, $T = 37$ °C.

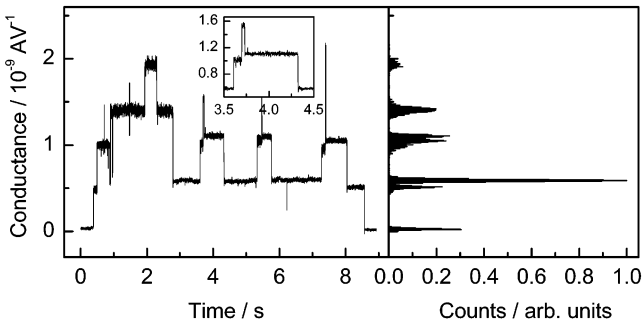

FIGURE 5: Current fluctuations after addition of 1.5 nM AP-B to the LPS side of a F515 LPS/PL bilayer at a clamp voltage of +25 mV. Left side, time course with inset (detail at higher resolution); right side, respective amplitude histogram. Bathing solution: 100 mM KCl, 5 mM $MgCl_2$, 8 mM NaCi, pH 5.2, $T = 37$ °C.

and it may be excluded that superimposition of several pores created this trace.

NK-lysin induced the formation of pores in both PL/PL (Figure 6 A) and F515 LPS/PL (Figure 6 B) membranes as well. However, the concentrations required for induction of a pore were significantly higher (by a factor of about 20) as compared to the concentrations needed to induce pores by amoebapores. In the case of PL/PL membranes (Figure 6 A), the pores appeared to have diameters of (0.45 ± 0.05) nm for positive and (0.40 ± 0.06) nm for negative clamp voltages. In F515 LPS/PL membranes, however, the NK-L pores had shorter lifetimes (about 1 ms) and larger diameters (about 1.9 nm). These pores could be induced by clamp voltages of 26 mV mimicking the potential of the outer membrane of Gram-negative bacteria.

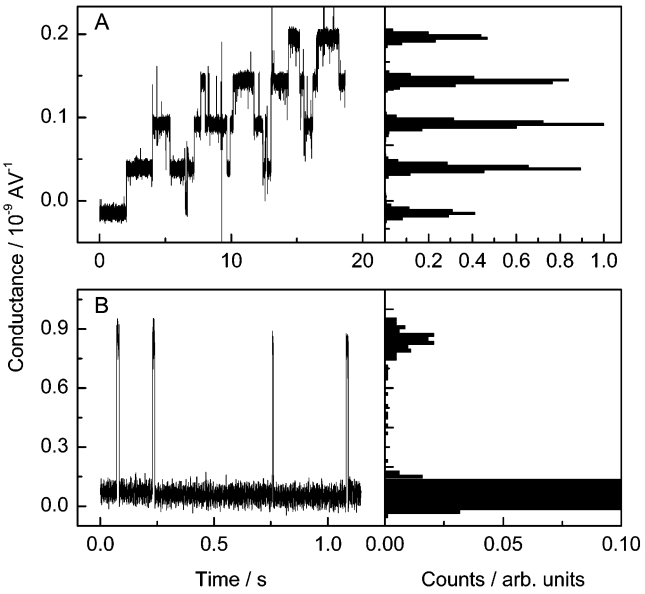

FIGURE 6: Current fluctuations after addition of 100 nM NK-L to (A) PL/PL at pH 5.2 and a clamp voltage of +60 mV and (B) F515 LPS/PL membranes at pH 7.0 and a clamp voltage of +50 mV. Left side, time course; right side, respective amplitude histogram. Bathing solution: 100 mM KCl, 5 mM $MgCl_2$, 5 mM HEPES, $T = 37$ °C.

Intercalation of the Peptides into Liposomes Composed of Lipopolysaccharide or Different Lipids. FRET spectroscopy is commonly used to investigate the intercalation of peptides/proteins into lipid membranes by monitoring changes of the energy transfer between two fluorescent markers. In contrast to the determination of single pore characteristics using the planar membranes, this technique averages over a large number of peptide molecules in membrane bilayers. All four peptides studied here showed a very weak intercalation into PC liposomes (data not shown) and a stronger intercalation into liposomes composed of negatively charged PS or of the polyanionic F515 LPS. As can be seen in Figure 7 A, NK-L but not AP-A intercalated strongly into F515 LPS liposomes at pH 7.0; however, at pH 5.2 both intercalated similarly. It is possible to compare the absolute values for the NK-L intercalation neither at different pH values nor from the PS and F515 LPS experiments because of a pH and lipid dependence of the liposome formation and the fluorescence properties of the dyes. The degree of intercalation of the three amoebapores showed the following order in both PS and F515 LPS liposomes: AP-A > AP-B > AP-C (Figure 7 B,C). It is important to mention that a change of the FRET signal is influenced by the amount of peptide, the depth of intercalation, and the size and orientation of the peptide in the membranes.

Monolayer Formation by the Peptides and Their Intercalation into Monolayers Made from PS or LPS. When amphiphilic or hydrophobic molecules are added to an aqueous phase (subphase), they tend to absorb to the air/water interface and, thus, reduce the surface tension of the

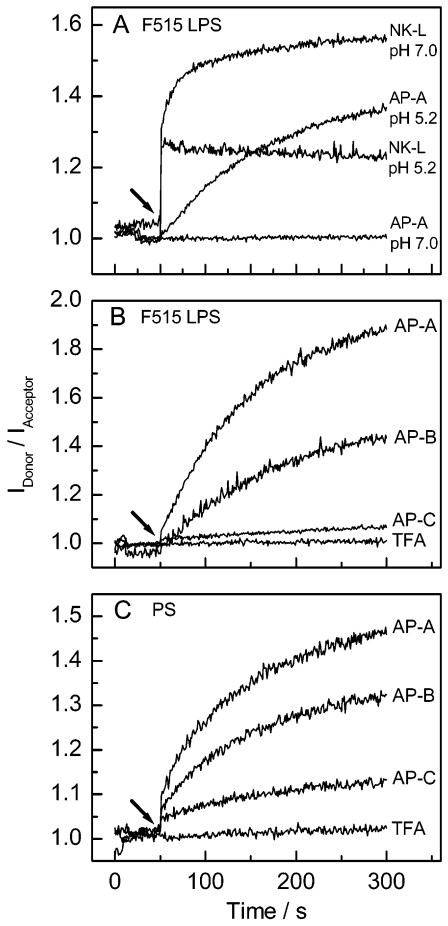

FIGURE 7: Changes of the FRET signal vs time after addition of 1 μg/mL peptide to 10 μM suspensions of (A and B) F515 LPS and (C) PS liposomes double-labeled with NBD-PE and Rh-PE. (A) Intercalation of AP-A and NK-L into F515 LPS liposomes at different pH. Bathing solutions: at pH 5.2, 100 mM KCl, 5 mM $MgCl_2$, 8 mM NaCi, $T = 37$ °C; at pH 7.0, 100 mM KCl, 5 mM $MgCl_2$, 5 mM HEPES, $T = 37$ °C. (B and C) Intercalation of AP-A, AP-B, and AP-C into F515 LPS and PS liposomes. Bathing solution: 100 mM KCl, 8 mM NaCi, pH 5.2, $T = 37$ °C. TFA was used as a control. Arrows mark time point of peptide additions.

subphase. The addition of AP-A and NK-L, which contain at least amphipathic segments in their structure, leads to the formation of peptide monolayers at the air/water interface as well. Compression of the AP-A and NK-L monolayers causes their collapse at a peptide specific lateral pressure of about 33 and 19 mN/m, respectively (Figure 8, traces a). Therefore, the areas occupied by one molecule of AP-A and NK-L at a lateral pressure of 18 mN/m, the highest lateral pressure up to which both monolayers were stable, are given in Table 1.

The addition of the peptides to the subphase beneath PS and F515 LPS monolayers at a constant lateral pressure of 20 mN/m led to an increase of the film area. From Figure 8 it can be deduced that peptides intercalated into the monolayers stayed in the lipid monolayer at the air/water interface even at higher lateral pressures as compared to the pure peptide monolayers. The isotherm in Figure 8A, trace c, shows that nearly no AP-A or AP-A/LPS complexes were displaced from the monolayer up to a lateral pressure of 40 mN/m. In contrast, NK-L or NK-L/LPS complexes were displaced from the monolayer at pressures above approximately 20 mN/m (Figure 8B, trace c).

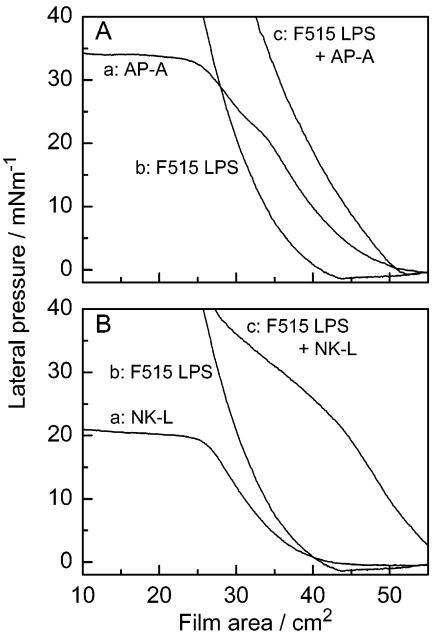

FIGURE 8: Pressure−area isotherms of pure AP-A and NK-L monolayers, pure F515 LPS monolayers, and F515 LPS monolayers after the intercalation of peptides. Traces a, isotherms of (A) AP-A and (B) NK-L monolayers on peptide suspensions; traces b, isotherm of F515 LPS monolayers; traces c, isotherms of F515 LPS monolayers after peptide addition to the subphase. Peptide concentrations: 50 ng/mL. Subphase: 100 mM KCl, 8 mM NaCi, pH 5.2, $T = 37$ °C.

Table 1: Molecular Areas Occupied by Amoebapores (AP) and by NK-Lysin (NK-L) in Pure Peptide Monolayers or Intercalated into PS or F515 LPS Monolayers[a]

	peptide monolayer, pH 5.2 A/nm^2	PS monolayer, pH 5.2 A/nm^2	PS monolayer, pH 7.0 A/nm^2	LPS monolayer, pH 5.2 A/nm^2
AP-A	22.0 ± 0.5	8.5 ± 1.2	3.7 ± 0.4	0.5 ± 0.1
AP-B	n.d.	12.4 ± 1.2	n.d.	7.7 ± 1.8
AP-C	n.d.	1.1 ± 0.2	n.d.	0
NK-L	15.1 ± 0.5[b]	11.8 ± 3.7	11.3 ± 1.2	12.9 ± 0.5

[a] The monolayers were prepared on two different subphases (bathing solutions): at pH 5.2, 100 mM KCl, 8 mM NaCi, $T = 37$ °C; at pH 7.0, 100 mM KCl, 5 mM HEPES, $T = 37$ °C. The areas of the peptides were determined at a lateral pressure of 20 mN·m^{-1}, except for those values marked with *b*. Here, the lateral pressure was 18 mN·m^{-1}.

In Figure 9, the increase in area after addition of each of the three amoebapore isoforms and of NK-L to the subphase of F515 LPS (Figure 9A) and of PS (Figure 9B) monolayers is presented. The areas given in Table 1 were calculated from at least three experiments using different peptide concentrations. With regard to amoebapores the order of the molecular areas occupied by the peptides is somewhat divergent from that derived from the FRET experiments: AP-B > AP-A > AP-C. The area occupied by a NK-L molecule was larger than those of the amoebapores. Apparently, the areas occupied by the amoebapore molecules are large in the case of PS monolayers on a subphase at pH 5.2, smaller in the case of PS monolayers on a subphase at pH 7.0 and smallest in the case of F515 LPS monolayers on a subphase at pH 5.2. In contrast to this, the size of NK-L did not depend on the lipid composition of the monolayer or the pH of the subphase.

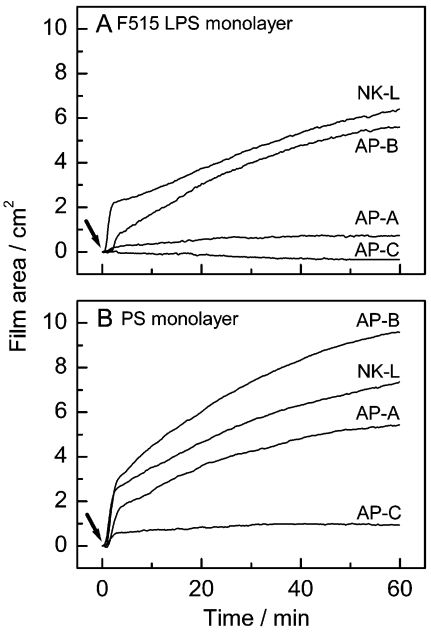

FIGURE 9: Increase in film area of (A) F515 LPS and (B) PS monolayers vs time at a constant lateral pressure of 20 mN/m after addition of 25 ng/mL AP-A, AP-B, AP-C, or NK-L to the subphase. Subphase 100 mM KCl, 8 mM NaCi, pH 5.2, $T = 37$ °C. Arrows mark time point of peptide additions.

DISCUSSION

The three isoforms of the amoebapores originating from the protozoon *Entamoeba histolytica* and the NK-lysin originating from porcine natural killer cells and cytotoxic lymphocytes exhibit antimicrobial activities, and the proposed mechanism of action is the permeabilization of membranes. However, a number of questions have arisen from previous studies, especially concerning the differences between amoebapores and NK-lysin in target cell preference, influence of pH on activity, and mechanism of membrane disruption. Accordingly, to us it seemed warranted to compare their membrane interaction in parallel by employing biophysical methods.

Characterization of Pores Induced by Amoebapores and NK-Lysin. The addition of AP-A, AP-B, AP-C, and NK-L to reconstituted planar lipid bilayers of various compositions, including DPhyPC/DPhyPC, PL/PL, and LPS/PL, caused in each combination a change in membrane capacitance (Figure 1). This behavior is indicative of an intercalation of the peptides into the membranes as shown earlier for peptides, e.g., cathelicidins (*34*). Furthermore, all peptides studied here led to the formation of membrane pores; the concentration needed was dependent on the interacting lipids and peptides. These data obtained from experiments on model membranes are consistent with the behavior of amoebapores and NK-lysin toward natural membranes (*2*, *7*, *12*).

In general, the amoebapores formed distinct pores with similar characteristics (size and lifetime) at similar peptide concentrations in PL/PL membranes (Figure 2). Pores with different sizes were also observed. The different sizes may be related to different sublevels of the pores due to conformational changes or to independent pores of different sizes. However, the repeating fluctuation patterns (see Figure 5) indicate that the formation of sublevels of individual pores leads to the different conductance levels. The pores are voltage-dependent. A negative polarity (side opposite to peptide addition is grounded) of the clamp voltage leads to higher conductances of the pores than a positive polarity (Figure 3). Thus, in the bacterial cell membrane, the amoebapores most likely form the smaller pores. The conductance at different negative clamp voltages is independent of its height; however, at higher clamp voltages the probability of the occurrence of sublevels increases.

It has been proposed that amoebapore belongs to the "barrel-stave" class of pore formers, in which channels are formed by progressive oligomerization of a more or less defined number of monomers around a central pore (*25*). The data presented in this paper show that amoebapore-induced pores in LPS/PL membranes have very different sizes and lifetimes (Figures 4 and 5) as compared to pores induced in PL/PL membranes. Thus, the pores have lipid-specific characteristics, and this specificity may result either from the formation of mixed lipid−peptide pores or a lipid-mediated organization of the peptides in the membrane. The formation of pores in the outer membrane is not sufficient to kill gram-negative bacteria. The peptides just pass the outer and reach the inner membrane. The induction of pores in the outer membrane might lead to a self-promoted uptake of amoebapore molecules. However, most of the pores are too small to allow the passage of further peptide molecules. Furthermore, the molecules forming the pores in the outer membrane are no longer available for antimicrobial action. Therefore, we propose that the observation that amoebapores are active against Gram-positive bacteria at lower concentrations than against Gram-negative bacteria may be explained by the additional permeabilization of the outer membrane in the latter case.

In previous studies, the dependence of amoebapores on acidic pH to display full activity has been described for several targets (*8*, *12*, *40*). However, we could not observe any effect of the pH on the characteristics of individual pores. Keller et al. (*25*) observed a higher open probability at higher pH with amoebic extracts, which is in contrast to the observation made here with the highly purified peptides and to the biological activities.

Besides the amoebapores, NK-lysin also causes the formation of pores with distinct characteristics. This is in contrast to results reported by Ruysschaert et al. showing that NK-lysin induces the formation of irregular pores in asolectin bilayers (*26*). Different results might arise from the use of different lipids or different membrane formation techniques. Membranes formed by using the Mueller−Rudin technique usually contain a higher amount of the solvent (*n*-decane) than the membranes used for the experiments presented in this work, which were reconstituted by the Montal−Mueller technique. Nonetheless, the NK-lysin concentrations necessary to induce pores in PL/PL and also in LPS/PL membranes are at least 20 times higher (Figure 6) as compared to the amoebapore concentrations. This is an indication that the aggregation/oligomerization process of NK-L in the buffer or, more likely, in the membrane is different to that of the three amoebapore isoforms. We did not observe any sublevels or pH dependence of the NK-L pores, but we did find lipid specificity with larger pore sizes in LPS/PL than in PL/PL bilayers (Figure 6).

Intercalation into Liposomes and Monolayers. The characteristics of the individual pores induced by amoebapore

isoforms can neither explain the observed pH-dependence nor target cell preferences (*12*). Thus, it is likely that not the individual pore is responsible for the specificities, but the interaction of an ensemble of peptide molecules with membranes. Therefore, we used liposome and monolayer techniques to get more insight into these specificities.

From both parameters, changes of the FRET-signal utilizing PS and F515 LPS liposomes as well as increase in the area of PS and F515 LPS monolayers, an intercalation of the amoebapores and of NK-L can be deduced (Table 1, Figures 7−9). However, the two parameters were differently affected by the three different isoforms. In the FRET experiments, we observed an order of decreasing intercalation from AP-A over AP-B to AP-C (Figure 7), and in the monolayer experiments the order of decreasing molecular areas is from AP-B over AP-A to AP-C. These differences between the results from the two methods may be due to the fact that the quality of the intercalation of the peptides, e.g., the depth of intercalation, into monolayers is different to that into liposomes. However, from these experiments it cannot be concluded directly that the three amoebapores intercalate into cell membranes in different ways. The monolayer experiments also revealed that the averaged area occupied by AP-A molecules in lipid monolayers is smaller than that in the pure peptide monolayer. Furthermore, the area occupied by one AP-A molecule at pH 5.2 is higher by more than a factor 2 than that at pH 7.0. The area occupied by each of the three isoforms in F515 LPS monolayers is smaller than in PS monolayers (Table 1), which is consistent with the observation that the amoebapores are less active against Gram-negative than against Gram-positive bacteria, the latter having a high content of PS in their membrane.

NK-L does not show a pH-dependence and is active at comparable concentrations against Gram-positive and against Gram-negative bacteria. Our finding that the areas occupied by NK-L in PS or in F515 LPS monolayers at different pH do not differ significantly (Table 1) is consistent with the reported comparable activities against Gram-positive and Gram-negative bacteria at neutral pH (*2*).

As already mentioned, in planar bilayer experiments, 20 times higher concentrations of NK-L as compared to the amoebapores were needed to induce pores. However, the results from monolayer and FRET experiments show that binding/intercalation of NK-L is comparable to that of the amoebapores. These concentration differences in pore formation and binding to the lipids support the suggested difference in the oligomerization process. The interpretation that the different concentrations required for the formation of pores by the amoebapores or NK-L is related to different oligomerization processes is also backed by the monolayer experiments (Figure 8). The pure AP-A monolayer is stable up to a lateral pressure of 33 mN/m, whereas the NK-L monolayer is stable only up to 19 mN/m, and also the mixed F515 LPS + NK-L monolayers are less stable than the F515 LPS + AP-A monolayers.

The first target of antimicrobial peptides is the (outer) membrane of the microbial organism. The initial interaction may already lead to the killing of the microorganism by destruction of the membrane. There are several examples in the literature of this mode of action (*34*, *41*). Another mode of action is the permeation of the membrane to allow the peptide to reach its final locus of action. This permeation might be accompanied by the (transient) disturbance of the bilayer integrity.

In summary, our data show that the three amoebapore isoforms and notably also NK-lysin induce the formation of pores with distinct characteristics, the sizes of which depend on the polarity and the probability of the occurrence of sublevels on the height of the applied voltage. The pores are lipid- but not pH-dependent. It should, however, be pointed out that not the individual pore but the capacity of the peptides to intercalate into lipid matrixes may well be responsible for the different activities of the amoebapores against Gram-negative and Gram-positive bacteria and also for the pH dependence.

ACKNOWLEDGMENT

We are indebted to Mrs. C. Hamann and Mr. D. Koch for performing the FRET and the film balance measurements, respectively. We thank Claudia Ott for the technical assistance during purification of amoebapores.

REFERENCES

1. Zasloff, M. (2002) Antimicrobial peptides of multicellular organisms, *Nature 415*, 389−395.
2. Andersson, M., Gunne, H., Agerberth, B., Boman, A., Bergman, T., Sillard, R., Jornvall, H., Mutt, V., Olsson, B., and Wigzell, H. (1995) NK-lysin, a novel effector peptide of cytotoxic T and NK cells. Structure and cDNA cloning of the porcine form, induction by interleukin 2, antibacterial and antitumour activity, *EMBO J. 14*, 1615−1625.
3. Pena, S. V., Hanson, D. A., Carr, B. A., Goralski, T. J., and Krensky, A. M. (1997) Processing, subcellular localization, and function of 519 (granulysin), a human late T cell activation molecule with homology to small, lytic, granule proteins, *J. Immunol. 158*, 2680−2688.
4. Leippe, M. (1995) Ancient weapons: NK-lysin is a mammalian homolog to pore-forming peptides of a protozoan parasite, *Cell 83*, 17−18.
5. Leippe, M., Ebel, S., Schoenberger, O. L., Horstmann, R. D., and Muller-Eberhard, H. J. (1991) Pore-forming peptide of pathogenic Entamoeba histolytica, *Proc. Natl. Acad. Sci. U.S.A. 88*, 7659−7663.
6. Leippe, M., Tannich, E., Nickel, R., van der, G. G., Pattus, F., Horstmann, R. D., and Müller-Eberhard, H. J. (1992) Primary and secondary structure of the pore-forming peptide of pathogenic Entamoeba histolytica, *EMBO J. 11*, 3501−3506.
7. Leippe, M., Andrä, J., Nickel, R., Tannich, E., and Müller-Eberhard, H. J. (1994) Amoebapores, a family of membraneolytic peptides from cytoplasmic granules of *Entamoeba histolytica*: isolation, primary structure, and pore formation in bacterial cytoplasmic membranes, *Mol. Microbiol. 14*, 895−904.
8. Andrä, J. and Leippe, M. (1994) Pore-forming peptide of Entamoeba histolytica. Significance of positively charged amino acid residues for its mode of action, *FEBS Lett. 354*, 97−102.
9. Munford, R. S., Sheppard, P. O., and O'Hara, P. J. (1995) Saposin-like proteins (SAPLIP) carry out diverse functions on a common backbone structure, *J. Lipid Res. 36*, 1653−1663.
10. Liepinsh, E., Andersson, M., Ruysschaert, J. M., and Otting, G. (1997) Saposin fold revealed by the NMR structure of NK-lysin, *Nat. Struct. Biol. 4*, 793−795.
11. Stenger, S., Hanson, D. A., Teitelbaum, R., Dewan, P., Niazi, K. R., Froelich, C. J., Ganz, T., Thoma-Uszynski, S., Melian, A., Bogdan, C., Porcelli, S. A., Bloom, B. R., Krensky, A. M., and Modlin, R. L. (1998) An antimicrobial activity of cytolytic T cells mediated by granulysin, *Science 282*, 121−125.
12. Andrä, J., Herbst, R., and Leippe, M. (2003) Amoebapores, archaic effector peptides of protozoan origin, are discharged into phagosomes and kill bacteria by permeabilizing their membranes, *Dev. Comp. Immunol. 27*, 291−304.
13. Leippe, M. (1997) Amoebapores, *Parasitol. Today 13*, 178−183.

14. Bruhn, H., and Leippe, M. (1999) Comparative modeling of amoebapores and granulysin based on the NK− lysin structure-structural and functional implications, *Biol. Chem. 380*, 1001−1007.
15. Vaara, M. (1992) Agents that increase the permeability of the outer membrane, *Microbiol. Rev. 56*, 395−411.
16. Nikaido, H., and Vaara, M. (1985) Molecular basis of bacterial outer membrane permeability, *Microbial. Rev. 49*, 1−32.
17. Osborn, M. J., Gander, J. E., Parisi, E., and Carson, J. (1972) Mechanism and assembly of the outer membrane of *Salmonella typhimurium*, *J. Biol. Chem. 247*, 3962−3972.
18. Kagan, B. L., Selsted, M. E., Ganz, T., and Lehrer, R. I. (1990) Antimicrobial defensin peptides form voltage-dependent ion-permeable channels in planar lipid bilayer membranes, *Proc. Natl. Acad. Sci. U.S.A. 87*, 210−214.
19. Wu, M., Maier, E., Benz, R., and Hancock, R. E. (1999) Mechanism of interaction of different classes of cationic antimicrobial peptides with planar bilayers and with the cytoplasmic membrane of *Escherichia coli*, *Biochemistry 38*, 7235−7242.
20. Dalla, S. M., and Menestrina, G. (2000) Characterization of molecular properties of pore-forming toxins with planar lipid bilayers, *Methods Mol. Biol. 145*, 171−188.
21. Gutsmann, T., Hagge, S. O., Larrick, J. W., Seydel, U., and Wiese, A. (2001) Interaction of CAP18-Derived Peptides with Membranes Made from Endotoxins or Phospholipids, *Biophys. J. 80*, 2935−2945.
22. Montal, M., and Mueller, P. (1972) Formation of bimolecular membranes from lipid monolayers and a study of their electrical properties, *Proc. Natl. Acad. Sci. U.S.A. 69*, 3561−3566.
23. Seydel, U., Schröder, G., and Brandenburg, K. (1989) Reconstitution of the lipid matrix of the outer membrane of Gram-negative bacteria as asymmetric planar bilayer, *J. Membr. Biol. 109*, 95−103.
24. Lynch, E. C., Rosenberg, I. M., and Gitler, C. (1982) An ion-channel forming protein produced by Entamoeba histolytica, *EMBO J. 1*, 801−804.
25. Keller, F., Hanke, W., Trissl, D., and Bakker-Grunwald, T. (1989) Pore-forming protein from *Entamoeba histolytica* forms voltage- and pH-controlled multi-state channels with properties similar those of the barrel-stave aggregates, *Biochim. Biophys. Acta 982*, 89−93.
26. Ruysschaert, J. M., Goormaghtigh, E., Homble, F., Andersson, M., Liepinsh, E., and Otting, G. (1998) Lipid membrane binding of NK-lysin, *FEBS Lett. 425*, 341−344.
27. Miteva, M., Andersson, M., Karshikoff, A., and Otting, G. (1999) Molecular electroporation: a unifying concept for the description of membrane pore formation by antibacterial peptides, exemplified with NK− lysin, *FEBS Lett. 462*, 155−158.
28. Wiese, A., Münstermann, M., Gutsmann, T., Lindner, B., Kawahara, K., Zähringer, U., and Seydel, U. (1998) Molecular mechanisms of Polymyxin B-membrane interactions: direct correlation between surface charge density and self-promoted uptake, *J. Membr. Biol. 162*, 127−138.
29. Galanos, C., Lüderitz, O., and Westphal, O. (1969) A new method for the extraction of R lipopolysaccharides, *Eur. J. Biochem. 9*, 245−249.
30. Nickel, R., Ott, C., Dandekar, T., and Leippe, M. (1999) Pore-forming peptides of Entamoeba dispar. Similarity and divergence to amoebapores in structure, expression and activity, *Eur. J. Biochem. 265*, 1002−1007.
31. Jacobs, T., Bruhn, H., Gaworski, I., Fleischer, B., and Leippe, M. (2003) NK-Lysin and Its Shortened Analog NK-2 Exhibit Potent Activities against Trypanosoma cruzi, *Antimicrob. Agents Chemother. 47*, 607−613.
32. Elman, G. L. (1959) Tissue sulfhydryl groups, *Arch. Biochem. Biophys. 82*, 70−77.
33. Wiese, A., and Seydel, U. (1999) Electrophysiological measurements on reconstituted outer membranes, *Methods Mol. Biol. 145*, 355−370.
34. Gutsmann, T., Larrick, J. W., Seydel, U., and Wiese, A. (1999) Molecular mechanisms of interaction of rabbit CAP18 with outer membranes of Gram-negative bacteria, *Biochemistry 38*, 13643−13653.
35. Jain, M. K., and Wagner, R. C. (1980) *Introduction to Biological Membranes*, John Wiley, New York.
36. Alvarez, O., and LaTorre, R. (1978) Voltage-dependent capacitance in lipid bilayers made from monolayers, *Biophys. J. 21*, 1−17.
37. Struck, D. K., Hoekstra, D., and Pagano, R. E. (1981) Use of resonance energy transfer to monitor membrane fusion, *Biochemistry 20*, 4093−4099.
38. Gutsmann, T., Fix, M., Larrick, J. W., and Wiese, A. (2000) Mechanisms of action of rabbit CAP18 on monolayers and liposomes made from endotoxins or phospholipids, *J. Membr. Biol. 176*, 223−236.
39. Sen, K., Hellman, J., and Nikaido, H. (1988) Porin channels in intact cells of *Escherichia coli* are not affected by Donnan potentials across the outer membrane, *J. Biol. Chem. 263*, 1182−1187.
40. Berninghausen, O., and Leippe, M. (1997) Necrosis versus apoptosis as the mechanism of target cell death induced by Entamoeba histolytica, *Infect. Immun. 65*, 3615−3621.
41. Harder, J., Bartels, J., Christophers, E., and Schröder, J. M. (2001) Isolation and characterization of human beta -defensin-3, a novel human inducible peptide antibiotic, *J. Biol. Chem. 276*, 5707−5713.

BI034686U